




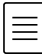
Title: SDS-induced oligomerization of **Myotoxin-II** from *Bothrops asper* assessed by sedimentation velocity and nuclear magnetic resonance.

Authors: Please add your affiliation and e-mail address

Abstract:

We report the solution behavior, oligomerization state, and structural details of Myotoxin-II purified from the venom of *Bothrops asper* in the presence and absence of sodium dodecyl sulfate (SDS) and multiple lipids, as examined by analytical ultracentrifugation and nuclear magnetic resonance. Molecular functional and structural details of the myotoxic mechanism of group II **Lys-49 phospholipases** have been only partially elucidated so far, and conflicting observations have been reported in the literature regarding the monomeric vs. oligomeric state of these toxins in solution. We observed the formation of a stable and discrete, large-molecular oligomeric form of Myotoxin-II, consistent with a hexamer  only in the presence of small amounts of SDS. In SDS-free medium, Myotoxin-II was insensitive to mass action and remained monomeric at all concentrations examined  (up to a 3 mg/ml). At SDS concentrations above the critical micelle concentration, **dimers and trimers**  were observed, and at **intermediate SDS concentrations**, aggregates larger than hexamers were observed. We found that the amount of SDS required to form a stable hexamer varies with protein concentration, suggesting the need for a precise stoichiometry of free SDS molecules. The discovery of a stable hexameric species **in the presence of a phospholipid mimetic** suggests a possible physiological role for this oligomeric form, and may shed light on the myotoxic mechanism of this protein class, such as pore formation or membrane disruption.

1. Introduction:

Myotoxin-II (MT-II) found in the venom of the snake *Bothrops asper* is a 121 residue toxin belonging to the **group II Lys-49 phospholipase A₂-like (PLA₂-like)** proteins which are present in many viperid species [1, 2]. In spite of being catalytically inactive, the Lys-49 PLA₂-like proteins induce a rapid skeletal muscle necrosis at the site of injection [3], which in severe envenoming cases may lead to permanent tissue damage or even amputations. The crystal structures of *B. asper* MT-II, alone (1CLP) or in complex with suramin (1Y4L) have been solved as homodimers, although with a different spatial arrangement of the monomers [4, 5]. **Its myotoxic effect has been shown to depend on a stretch of amino acids at its C-terminal region, which combines cationic and hydrophobic residues [6].** However, the molecular details of its mechanism of action are still poorly understood. **There have been conflicting observations about the solution behavior of MT-II.** The oligomerization properties of a different Lys-49 PLA₂ originating from *Protobothrops flavoviridis* have previously been investigated in the presence and absence of 1% sodium dodecyl sulfate (SDS) by native mass **spectroscopy**, analytical ultracentrifugation (AUC) and SDS-polyacrylamide gel electrophoresis (SDS-PAGE), as well as under oxidized and reducing conditions with **2-mercapto ethanol**, under denaturing conditions with urea, and before and after 95°C heat treatment [2]. The results showed that the *P.fl*-Lys-49 PLA₂ is monomeric in the absence of SDS, but one or more oligomeric species consistent with dimers and trimers were observed in all cases where SDS was present, although the relative amount of each oligomeric species varied, depending on the presence or absence of urea or reductant. The oligomerization behavior in response to SDS is unexpected since SDS is a detergent that acts as a strong protein denaturant, which is known to disrupt oligomeric structures of proteins. Typically, SDS-PAGE reports the monomeric molar mass, which was not observed with *P.fl*-Lys-49 PLA₂. 

To shed further light on the structural role of SDS as an inducer of oligomerization of MT-II, we examined the solution behavior of this protein by AUC and nuclear magnetic resonance (NMR) in the presence and absence of SDS and other lipids, and as a function of the protein and SDS concentration. We also attempted to determine the stoichiometry for the SDS:protein interaction. Non-covalent, reversible oligomerization is a common protein behavior, and any response to mass action needs to be considered whenever oligomerization is observed. Oligomerization as a response to mass action or a change in solution conditions, such as pH, ionic strength, reduction potential, or presence of chaotropes, denaturants, and other molecules present in the buffer, can be readily measured by AUC. AUC reports the sedimentation and diffusion coefficients, as well as the partial concentration of all molecules in the solution. If the partial specific volume is known, the sedimentation and diffusion coefficients can be transformed to molar mass and the degree of globularity. NMR further informs about the structural details that may be affected in the presence of a denaturant such as SDS. We attempted to define a stoichiometry of SDS binding for the oligomerization of Myotoxin-II in the presence of SDS, and measured this dependence on protein concentration.

2. Methods:

2.1 Myotoxin preparation:

Myotoxin II (UniProt code P24605) [1] was isolated from crude *Bothrops asper* venom by cation exchange chromatography on CM-Sephadex C25, followed by RP-HPLC, as previously described [7, 8]. Homogeneity of the protein was confirmed by mass spectrometry using direct infusion in a Q-Exactive Plus instrument (Thermo) [9].

2.2 Analytical Ultracentrifugation:

Oligomerization properties of MT-II were studied by sedimentation velocity (SV) as a function of SDS and protein concentration. Sedimentation experiments were performed on a Beckman Optima AUC instrument at the Canadian Center for Hydrodynamics at the University of Lethbridge. Samples were measured at 20°C and 55 krpm by UV intensity detection using an An60Ti rotor and standard 2-channel epon-filled centerpieces (Beckman-Coulter, Indianapolis). All data were analyzed with UltraScan 4.0 release 6485 [10, 11]. All samples were measured in a 10 mM sodium phosphate buffer containing 50 mM NaCl, pH 7.4. Hydrodynamic buffer density (1.0012 g/cm³) and viscosity (1.0065 cp) were estimated with UltraScan [10]. Sedimentation velocity (SV) data were analyzed as reported earlier [12]. Optimization was performed by 2-dimensional spectrum analysis (2DSA) [13, 14] with simultaneous removal of time- and radially invariant noise contributions and fitting of boundary conditions. Where appropriate, 2DSA solutions were subjected to parsimonious regularization by genetic algorithm analysis [15]. Diffusion-corrected integral sedimentation profiles were generated with the enhanced van Holde–Weischet analysis [16]. A further refinement using Monte Carlo analysis [17] was also applied to determine confidence limits for the determined parameters. The calculations were carried out on high-performance computing platforms at the Texas Advanced Computing Center and the San Diego Supercomputing Center and on the cluster from the Canadian Center for Hydrodynamics [18].

2.3 Nuclear Magnetic Resonance:

Paul...

3. Results:

3.1 Myotoxin-II Purification:

Deconvolution of the multicharged ion series of intact MT-II analyzed by high-resolution ESI-MS showed a monoisotopic mass of 13750.52 Da (see SI 1), in agreement with its amino acid sequence (P24605). Protein homogeneity above 95% was estimated by fractional abundance analysis.

3.2 Analytical Ultracentrifugation:

To examine the oligomeric configuration of MT-II, we initially measured the sedimentation and diffusion profiles derived from sedimentation velocity experiments of MT-II at four different protein concentrations (0.031 mg/ml, 0.48 mg/ml, 2.0 mg/ml, and 3.0 mg/ml) in a buffer containing 40 mM sodium phosphate and 120 mM NaCl at pH 7.2. The results showed that MT-II's oligomerization state did not change over this concentration range, even at the highest concentration measured (see Figure 1). Using a global genetic algorithm-Monte Carlo analysis over all concentrations, we determined the sedimentation (s) and diffusion coefficient (D) of MT-II in the absence of SDS (see Table 1). Together with the sedimentation and diffusion coefficients, and the measured molar mass (M) from the mass spectrometry results of MT-II [19], we derived a partial specific volume (\bar{v}) of 0.725 ml/g by re-arranging the Svedberg equation (see Equ. 1), which compares very well with the sequence-derived partial specific volume of 0.726 ml/g as calculated by UltraScan.

$$\bar{v} = \frac{1}{\rho} \left(1 - \frac{sRT}{DM} \right)$$

Equ. 1

where ρ is the density of solvent, R is the universal gas constant, and T the temperature in Kelvin. We also calculated a frictional ratio of 1.15 for monomeric MT-II, which compares the measured frictional coefficient of the MT-II molecule, f , to the hypothetical minimal frictional coefficient of a sphere (f_0) with the same molar mass and partial specific volume. The frictional coefficient is readily obtained from the diffusion coefficient (see Equ. 2), and the volume of the sphere (V) can be obtained from the partial specific volume and the molar mass of MT-II (see Equ. 3), where N is Avogadro's number. Using the Stokes-Einstein relationship, a minimal frictional coefficient, f_0 , can be derived from the radius, r_0 , of the minimal sphere, and viscosity η (see Equ. 4 and Equ. 5).

$$f = \frac{RT}{ND}$$

Equ. 2

$$V = \frac{M\bar{v}}{N} = \frac{4}{3} \pi r_0^3$$

Equ. 3

$$r_0 = \left(\frac{3M\bar{v}}{4\pi N} \right)^{1/3}$$

Equ. 4

$$f_0 = 6\pi\eta r_0$$

Equ. 5

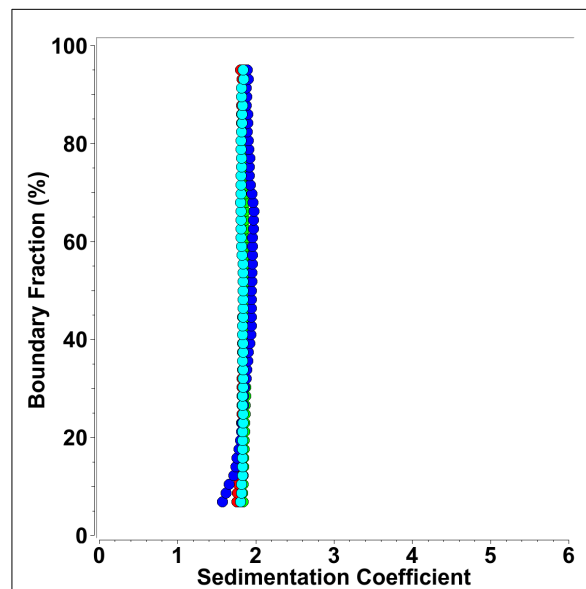


Figure 1: Diffusion-corrected van Holde - Weischet integral sedimentation coefficient distributions of multiple concentrations of MT-II (blue: 0.031 mg/ml, green: 0.48 mg/ml, red: 2.0 mg/ml, cyan: 3.0 mg/ml) generate homogeneous, identical sedimentation coefficient distributions, demonstrating the absence of mass action, reflecting a pure monomeric species.

Finally, we used the Zeno simulation routine in UltraScan-SOMO [20, 21] to predict sedimentation and diffusion coefficients for the monomer unit in the protein structure database pdb entry for *B.a*-Lys49-PLA₂ [22], which are in excellent agreement with the measured values, confirming that MT-II is monomeric over a large concentration range. The results are summarized in Table 1:

Table 1: *Hydrodynamic measurements of Myotoxin-II derived from a global genetic algorithm – Monte Carlo analysis in the absence of SDS.*

Hydrodynamic Parameter	Mean Value (from GA-MC)	95% confidence interval	US-SOMO
Sedimentation coefficient ($s_{20,w}$):	1.83e-13	(1.79e-13, 1.88e-13)	1.81e-13
Diffusion coefficient ($D_{20,w}$):	1.18e-06	(1.07e-06, 1.28e-06)	1.12e-06
Frictional Ratio:	1.15e+00	(1.08, 1.22)	1.22
Molar mass (Da, from mass spec):	13759.08	See: [19]	
Partial Specific Volume (ml/g):	0.725	(0.726 from sequence)	

Next, we investigated the oligomerization state of MT-II in the presence of SDS. SDS is a detergent with strong protein denaturant properties. However, as reported earlier in [3] for a related snake toxin, our results also demonstrate that SDS induces oligomerization of MT-II. Interestingly, the oligomerization behavior is highly sensitive to the protein-SDS ratio; the same protein-SDS ratio produces different results when the concentrations are changed, suggesting a specific stoichiometry of association has to be satisfied for each assembly state. Nevertheless, a consistent pattern of self-association was observed that was independent of total protein concentration. We started at a protein concentration of $\sim 24 \mu\text{M}$, monitored at 280 nm by SV, and titrated SDS from 0.001% to 0.5% (see Figure 2). The addition of SDS at very small concentrations leads to the formation of a well-defined, discrete **5.5 s species**. The amount of this oligomer formed appears to be proportional to the (limiting) amount of SDS added to the protein. At approximately 0.008% SDS, all monomeric MT-II has been complexed by SDS, forming the 5.5 s species. If the SDS concentration is lowered, an increasing portion of the MT-II signal remains monomeric. The transition is highly cooperative, demonstrating a sedimentation coefficient transition pattern that suggests a strong self-association with a low K_d . If the SDS concentration is increased further, the 5.5 s species is disrupted, and larger aggregates form, reaching up to 8.5 s. The precise composition in this range is very sensitive to small changes in SDS concentration. When the concentration is further increased to 0.1 % SDS, these aggregates are broken up into smaller species that range between **3-4 s**. At 0.5% SDS concentration, only MT-II dimers and trimers appear with s-values between 2.2-2.8 s, which matches the observations reported in [3] for *P.fl*-Lys-49 PLA₂ in 1% SDS. It should be noted that the critical micelle concentration (CMC) of SDS is approximately 8.3 mM SDS ($\sim 0.24\%$) [23]. The transition from monomeric MT-II to the stable 5.5 s species appears to be highly coordinated and dependent on the exact SDS

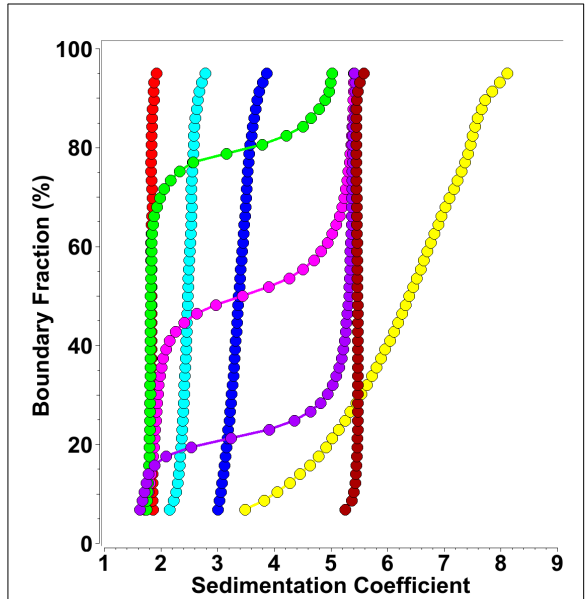


Figure 2: Diffusion corrected integral sedimentation coefficient distributions from SDS-MT-II titrations at $\sim 24 \mu\text{M}$ MT-II concentration (measured at 280 nm) and SDS concentrations variable between 0.001-0.5%. Red: 0.001%, green: 0.002 %, magenta: 0.003%, purple: 0.004%, dark red: 0.008%, yellow 0.05%, blue: 0.1%, cyan: 0.5%

concentration. Given the 13.68 μM MT-II concentration, this ratio of protein:SDS appears to be in the range of 20 SDS molecules per protein molecule. To examine if this protein:SDS ratio can be replicated at different protein concentrations, we performed additional protein:SDS titrations at different MT-II concentrations. In the analytical ultracentrifuge, it is trivial to change the detection wavelength in order to exploit significant differences in the protein's molar extinction coefficient. This extends the concentration range where a protein can be monitored. In our approach, we monitored MT-II sedimentation at 220 nm (using a $\sim 1.1 \mu\text{M}$ loading concentration) and 225 nm (using a $\sim 3.2 \mu\text{M}$ loading concentration), in each case performing titrations with SDS that replicated the observed pattern. The observed results for 220 nm are shown in Figure 4, and the results for 225 nm are shown in Figure 3. At 220 nm, we observed s-values below 1.0 s, which were attributed to SDS micelles, as a 220 nm experiment of a 1.0% SDS solution showed (see Figure 4). A transition to a 5.5 s species was apparent at SDS concentrations as low as 0.001%. Over 80% of MT-II sedimented at 0.0016% as a 5.5 s species.

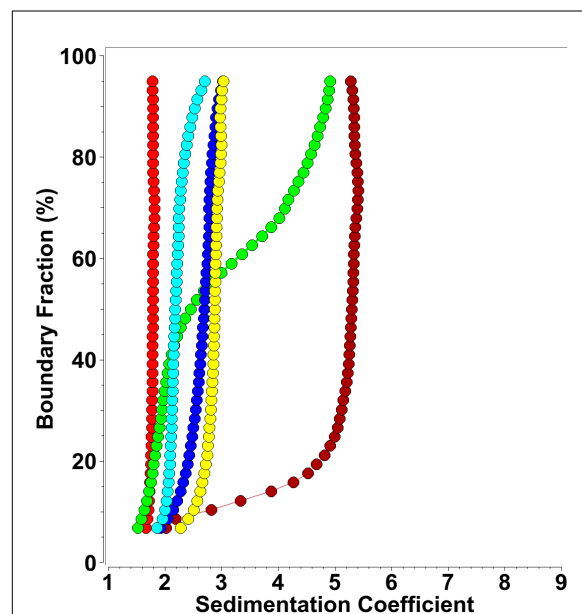


Figure 3: Diffusion corrected integral sedimentation coefficient distributions from SDS-MT-II titrations at $\sim 3.2 \mu\text{M}$ protein concentration (measured at 225 nm) and SDS concentrations variable between 0.0008-0.5%. Red: 0.0%, green: 0.0008 %, dark red: 0.0013%, yellow 0.05%, blue: 0.1%, cyan: 0.5%

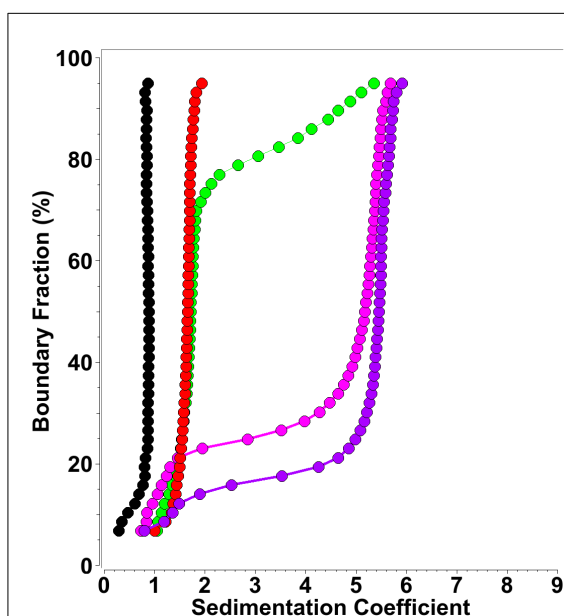


Figure 4: Diffusion corrected integral sedimentation coefficient distributions from SDS-MT-II titrations at $\sim 1.1 \mu\text{M}$ protein concentration (measured at 220 nm) and SDS concentrations variable between 0.0-0.0016%. Red: 0.0%, green: 0.001 %, magenta: 0.0015%, purple: 0.0016%, black: 1% SDS control, showing 0.9 S micelle sedimentation at 220 nm, explaining s-values below 1.0 S in samples with SDS.

Measurements at 225 nm produced a very similar picture. A small amount of MT-II was converted to the 5.5 s species at 0.0008 % SDS, while a 80% conversion to the 5.5 s species was observed at 0.0016% SDS. Increasing the SDS concentration to 0.05% produced primarily a 2.9 s species, while 0.1% SDS concentration resulted in a mixture sedimenting between 2.0 and 2.9 s, and a 0.5% SDS concentration produced the previously observed mixture of dimers and trimers. To test if other lipids or detergents produce similar discrete oligomerization behavior, we repeated titration measurements of MT-II in the presence of the following lipids and detergents: 1-myristoyl-2-hydroxy-sn-glycero-3-phospho-(1'-rac-glycerol) (LMPG), 1-palmitoyl-2-hydroxy-sn-glycero-3-phospho-(1'-rac-glycerol) (LPPG), 1-myristoyl-2-hydroxy-sn-glycero-3-phosphocholine (LMPC), 1-palmitoyl-2-hydroxy-sn-glycero-3-phosphocholine (LPPC), 1-(10Z-heptadecenoyl)-sn-glycerol-3-phospho-(1'-rac-glycerol) (LSPG), CYMAL-5, n-Undecyl- β -D-Maltoside (U300LA), sodium

dodecanoyl sarcosine (Sarcosyl), ω -undecylenyl- β -D-maltopyranoside (U310), and n-dodecyl- β -D-maltopyranoside (D310LA). Each lipid was measured at two or three concentrations below the CMC. Unlike SDS, none of these lipids measured in the presence of MT-II induced any oligomerization. These results are shown in SI 2-SI 10, where for each lipid or detergent the integral sedimentation coefficient distributions are overlaid for all concentrations measured.

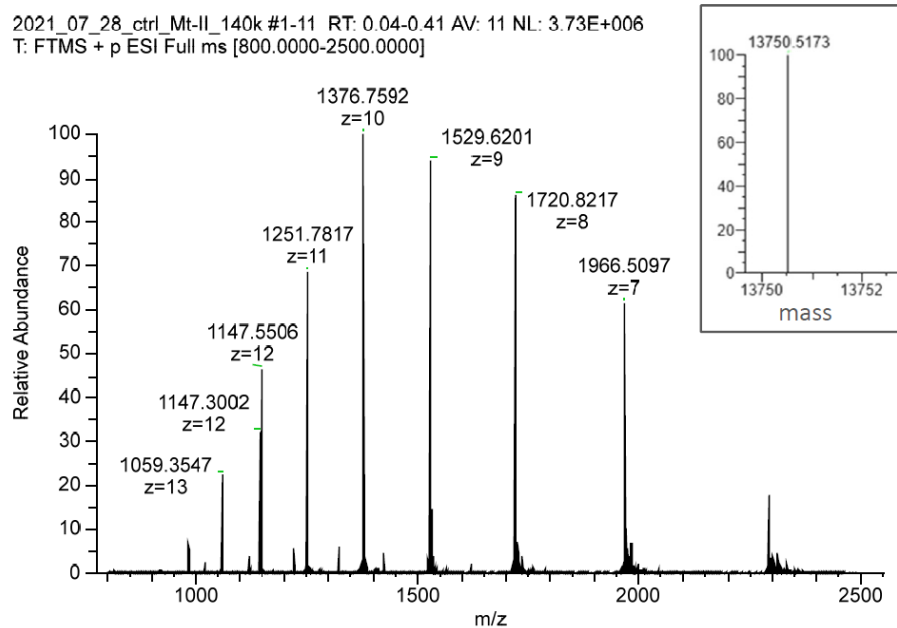
3.3 Nuclear Magnetic Resonance Spectroscopy:

4. Discussion:

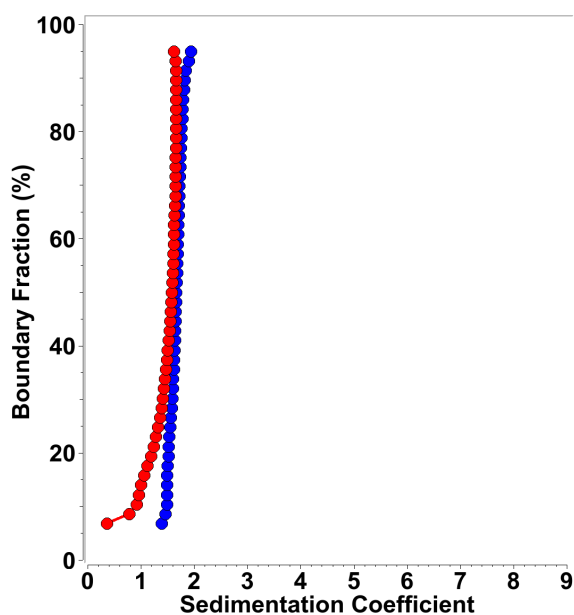
5. Acknowledgments:

We thank Dr. Sebastien Poget (State University New York) and Dr. Bruce Bowler (University of Montana) for providing lipids and detergents used in the analytical ultracentrifugation experiments. This work was supported by the Canada 150 Research Chairs program (C150-2017-00015, BD), the Canada Foundation for Innovation (CFI-37589, BD), the National Institutes of Health (1R01GM120600, BD) and the Canadian Natural Science and Engineering Research Council (DG-RGPIN-2019-05637, BD). UltraScan supercomputer calculations were supported through NSF/XSEDE grant TG-MCB070039N (BD), and University of Texas grant TG457201 (BD). The Canadian Natural Science and Engineering Research Council supports AH through a scholarship grant.

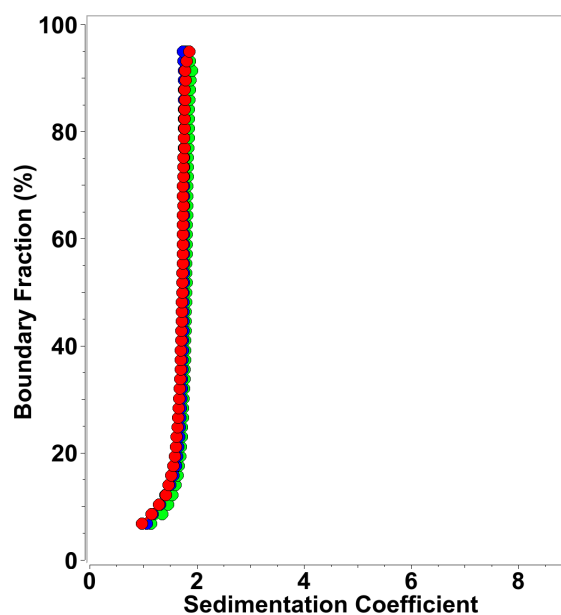
Supplemental Information



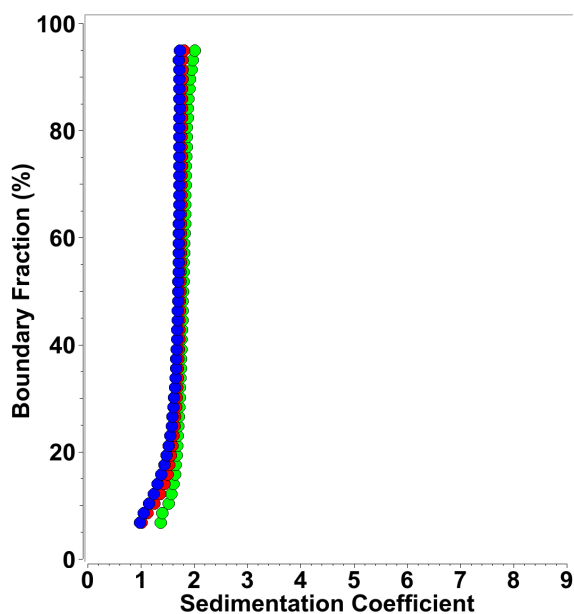
SI 1: ESI-MS analysis of MT-II showing its monoisotopic mass (inset).



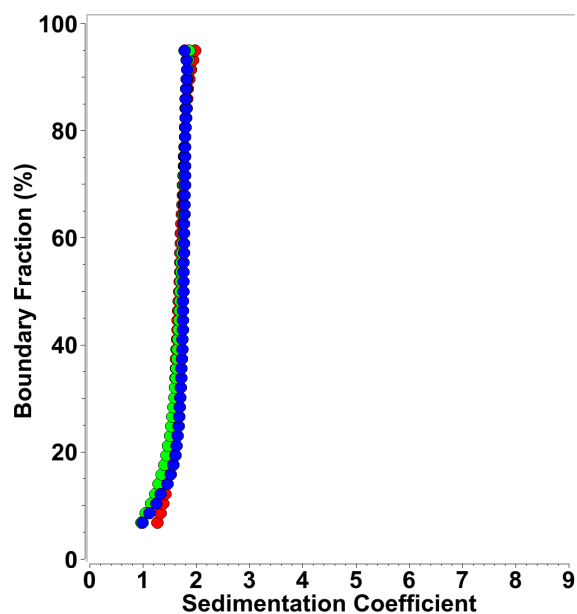
SI 2: Integral sedimentation coefficient distribution for MT-II in Sarcosyl. Blue: 3.6 mM, red: 26 μ M.



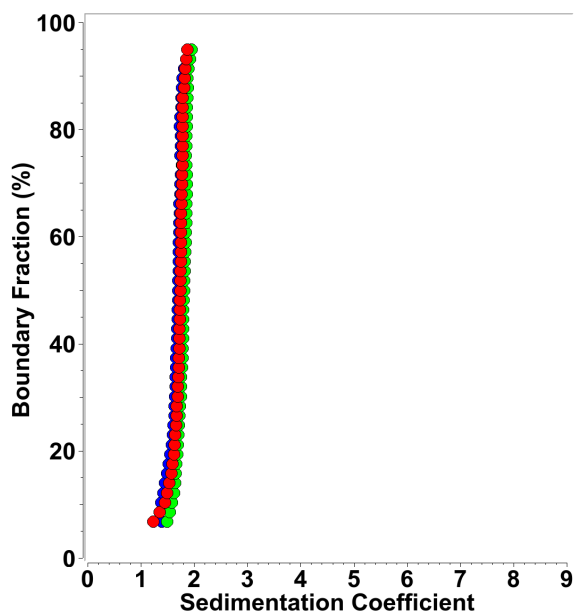
SI 3: Integral sedimentation coefficient distribution for MT-II in CYMAL-5. Blue: 0.9 mM, green: 2 mM, red: 26 μ M.



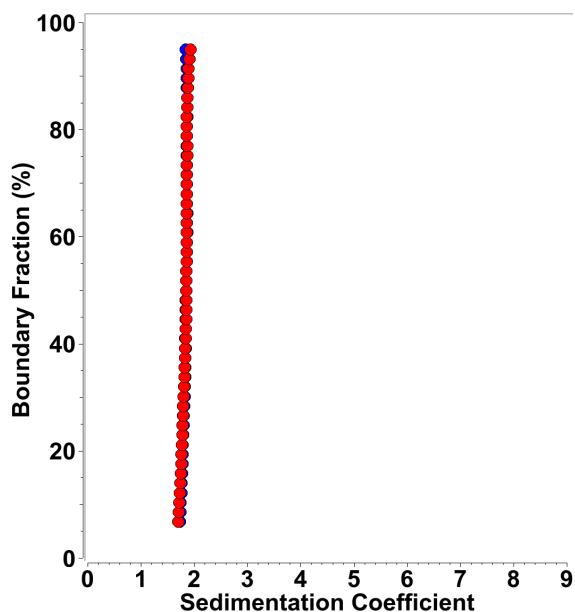
SI 4: Integral sedimentation coefficient distribution for MT-II in U300LA. Red: 0.3 mM, green: 0.59 mM, red: 26 μ M.



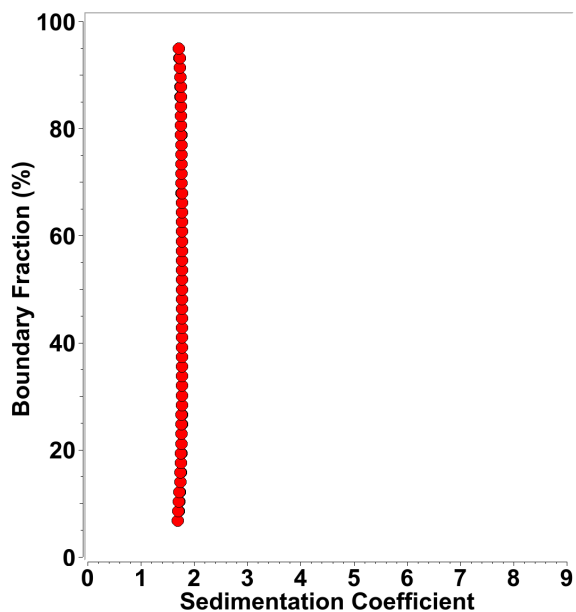
SI 5: Integral sedimentation coefficient distribution for MT-II in U310. Blue: 0.6 mM, green: 1.2 mM, red: 26 μ M.



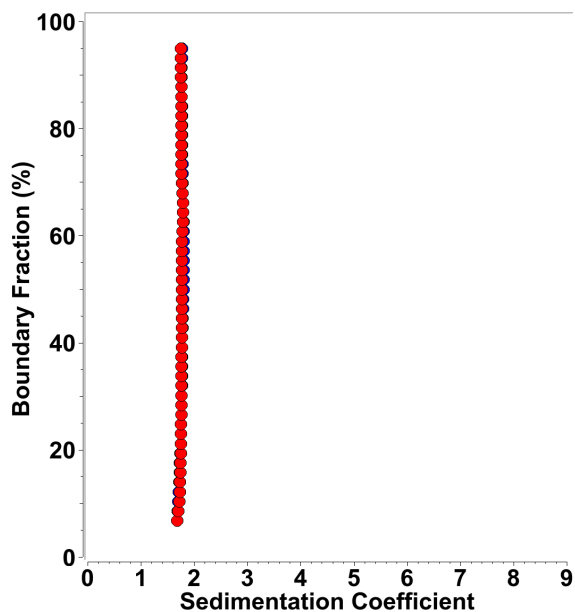
SI 6: Integral sedimentation coefficient distribution for MT-II in D310LA. Blue: 0.6 mM, green: 1.2 mM, red: 26 μ M.



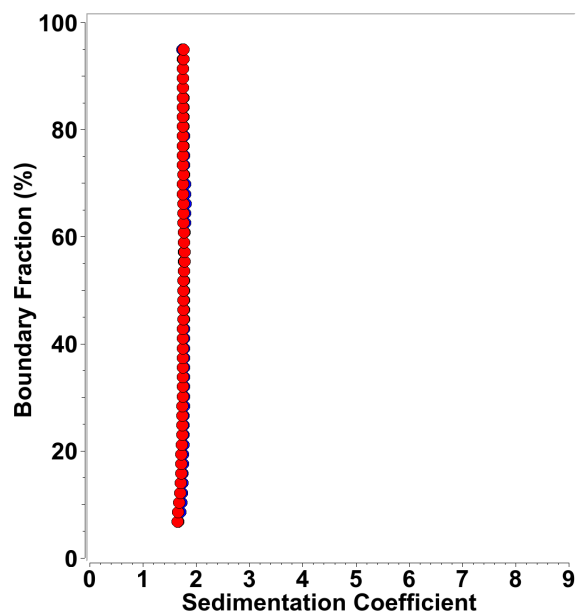
SI 7: Integral sedimentation coefficient distribution for MT-II in LMPG. Blue: 26 μ M, red: 52 μ M.



SI 8: Integral sedimentation coefficient distribution for MT-II in LPPG. Blue: 26 μ M, red: 52 μ M.



SI 9: Integral sedimentation coefficient distribution for MT-II in LPPC. Blue: 26 μ M, red: 52 μ M.



SI 10: Integral sedimentation coefficient distribution for MT-II in LSPG. Blue: 26 μM , red: 52 μM .

- 1 Francis B, Gutierrez JM, Lomonte B, Kaiser II. Myotoxin II from *Bothrops asper* (Terciopelo) venom is a lysine-49 phospholipase A₂. Arch Biochem Biophys. 1991 Feb 1;284(2):352-9. doi: 10.1016/0003-9861(91)90307-5. PMID: 1899180.
- 2 Matsui T, Kamata S, Ishii K, Maruno T, Ghanem N, Uchiyama S, Kato K, Suzuki A, Oda-Ueda N, Ogawa T, Tanaka Y. SDS-induced oligomerization of Lys49-phospholipase A₂ from snake venom. Sci Rep. 2019 Feb 20;9(1):2330. doi: 10.1038/s41598-019-38861-8. PMID: 30787342; PMCID: PMC6382788.
- 3 Lomonte B, Rangel J (2012) Snake venom Lys49 myotoxins: from phospholipases A₂ to non-enzymatic membrane disruptors. Toxicon 60, 520-530. DOI: 10.1016/j.toxicon.2012.02.007
- 4 Arni RK, Ward RJ, Gutiérrez JM, Tulinsky A (1995) Structure of a calcium-independent phospholipase-like myotoxic protein from *Bothrops asper* venom. Acta Cryst. D 51, 311–317.
- 5 Murakami MT, Arruda EZ, Melo PA, Martinez AB, Calil-Elias S, Tomaz MA, Lomonte B, Gutiérrez JM, Arni RK (2005) Inhibition of myotoxic activity of *Bothrops asper* myotoxin II by the anti-trypanosomal drug suramin. J. Mol. Biol. 350, 416-426.
- 6 Lomonte B, Moreno E, Tarkowski A, Hanson LÅ, Maccarana M (1994c) Neutralizing interaction between heparins and myotoxin II, a Lys-49 phospholipase A₂ from *Bothrops asper* snake venom. Identification of a heparin-binding and cytolytic toxin region by the use of synthetic peptides and molecular modeling. J. Biol. Chem. 269, 29867-29873.
- 7 Lomonte B, Gutiérrez JM (1989) A new muscle damaging toxin, myotoxin II, from the venom of the snake *Bothrops asper* (terciopelo). Toxicon 27, 725–733.
- 8 Mora-Obando D, Díaz C, Angulo Y, Gutiérrez JM, Lomonte B (2014a) Role of enzymatic activity in muscle damage and cytotoxicity induced by *Bothrops asper* Asp49 phospholipase A₂ myotoxins: are there additional effector mechanisms involved? Peer J. 2, e569. doi: 10.7717/peerj.569
- 9 Lomonte B, Fernández J. Solving the microheterogeneity of *Bothrops asper* myotoxin-II by high-resolution mass spectrometry: Insights into C-terminal region variability in Lys49-phospholipase A₂ homologs. Toxicon. 2022 Apr 30;210:123-131. doi: 10.1016/j.toxicon.2022.02.024. Epub 2022
- 10 Demeler, B., and Gorbet, G.E. (2016). "Analytical Ultracentrifugation Data Analysis with UltraScan-III," in *Analytical Ultracentrifugation*, eds. S. Uchiyama, F. Arisaka, W. Stafford & T. Laue. (Tokyo: Springer), 119-143.
- 11 Demeler B, Brookes EH, Gorbet GE, Savelyev A, Zollars D, Dubbs B. UltraScan Data Analysis Software for Analytical Ultracentrifugation Experiments and Hydrodynamic Modelling. 2022, <https://www.ultrascan.aucsolutions.com>
- 12 Demeler, B Methods for the Design and Analysis of Sedimentation Velocity and Sedimentation Equilibrium Experiments with Proteins. Cur. Protoc. Prot. Sci. 2010, Chapter 7 : Unit 7.13.
- 13 Brookes EH, Cao W, Demeler B. A two-dimensional spectrum analysis for sedimentation velocity experiments of mixtures with heterogeneity in molecular weight and shape. Eur. Biophys. J. 2010, 39, 405-414
- 14 Brookes EH, Boppana RV, Demeler B. Computing Large Sparse Multivariate Optimization Problems with an Application in Biophysics. Supercomputing '06 ACM. 0-7695-2700-0/06, 2006.
- 15 Brookes, E. H., and B. Demeler. Parsimonious Regularization using Genetic Algorithms Applied to the Analysis of Analytical Ultracentrifugation Experiments. GECCO Proceedings ACM. 2007. 978-1-59593-697-4/07/0007.
- 16 Demeler, B. and K. E. van Holde. Sedimentation velocity analysis of highly heterogeneous systems. Anal. Biochem. 2004. Vol 335(2):279-288
- 17 Demeler, B. and E. H. Brookes. Monte Carlo analysis of sedimentation experiments. Colloid Polym. Sci. 2008. 286:129-137
- 18 Brookes E, Demeler B. Parallel computational techniques for the analysis of sedimentation velocity experiments in UltraScan. Colloid Polym. Sci. 2008, 286, 138-148

- 19 Lomonte B, Fernández J. Solving the microheterogeneity of Bothrops asper myotoxin-II by high-resolution mass spectrometry: Insights into C-terminal region variability in Lys49-phospholipase A2 homologs. *Toxicon*. 2022 Apr 30;210:123-131. doi: 10.1016/j.toxicon.2022.02.024. Epub 2022 Mar 3. PMID: 35248586.
- 20 Brookes E, Demeler B, Rocco M. Developments in the US-SOMO bead modeling suite: new features in the direct residue-to-bead method, improved grid routines, and influence of accessible surface area screening. *Macromol Biosci*. 2010 Jul 7;10(7):746-53. doi: 10.1002/mabi.200900474. PMID: 20480513.
- 21 Brookes, E., Rocco, M. Recent advances in the UltraScan Solution MOdeller (US-SOMO) hydrodynamic and small-angle scattering data analysis and simulation suite. *Eur Biophys J* **47**, 855–864 (2018). <https://doi.org/10.1007/s00249-018-1296-0>
- 22 Arni RK, Gutiérrez JM. Crystallization and preliminary diffraction data of two myotoxins isolated from the venoms of Bothrops asper (Terciopelo) and Bothrops nummifer (jumping viper). *Toxicon*. 1993 Aug;31(8):1061-4. doi: 10.1016/0041-0101(93)90264-j. PMID: 8212044.
- 23 Cifuentes A, Bernal JL, Diez-Masa JC. Determination of Critical Micelle Concentration Values Using Capillary Electrophoresis Instrumentation. *Anal. Chem*. 1997, 69, 4271-4274